



Karaj branch

Application of Semiconductor Photocatalysis for Effective Elimination of Organic Contaminants from Sewage

Soodabe Gharibe

Department of Science, Firoozkooh Branch, Islamic Azad University, Firoozkooh, Iran

(Received 15 Sep. 2017; Final version received 18 Dec. 2017)

Abstract

The ZnO/SiO₂ semiconductor nanophotocatalysis was synthesized *via* sol-gel method. Also, the platinum particles were loaded on the ZnO/SiO₂ nanoparticles by photoreductive method. The structure of catalyst was confirmed by X-ray diffraction (XRD), scanning electron microscopy (SEM) and fourier transform infrared spectroscopy (FT-IR). The XRD patterns of ZnO particles displayed the nanoparticles have a wurtzite structure (hexagonal phase). The crystallite sizes were calculated using Scheerer's equation and were around 32nm. For photocatalytic test, decomposition of Malachite Green oxalate (MG), as an organic pollutant was carried out by synthesized catalyst. A comparison of degradation between bare catalyst and platinum loaded ZnO/SiO₂ nanoparticle under UV-Vis light irradiation shows that the Pt-ZnO/SiO₂ photocatalyst is more efficient than ZnO/SiO₂ nanoparticles. Also, the activity of ZnO/SiO₂ nanoparticles in the visible light are minimal, while loading of Pt in zinc oxide network displaced the band gap toward longer wavelengths (visible light) and increased the photocatalysis activity of ZnO/SiO₂ in the range of visible light.

Key words: *photocatalyst, Malachite Green, UV-Vis, ZnO, Organic pollutants.*

Introduction

The photocatalysis has focused on the employing of semiconductor materials as photocatalysts for elimination of organic and inorganic compounds from aqueous or gas media because of environmental and drinking water cleanup, industrial and health applications. The semiconductors with nano scale such as ZnO and TiO₂ are one of the important materials which have utilized as useful photocatalyst compounds [1-5]. Explanation of semiconductors such as ZnO and TiO₂ with photons of energies greater than the band gap energy puts on transitions electrons from the valence band to the transmission band by leaving behind positive holes. The valence band potential is enough positive to produce hydroxyl radicals at the semiconductor surface. Also, the transmission band potential is enough negative to decrease molecular O₂. The hydroxyl radical or hole(h⁺) is a powerful oxidant and absorbed organic pollutants that are existed at or near the surface of semiconductor photocatalysts and in complete oxidation converted to CO₂[6-9].

Elimination of organic pollutants that remain for a long time in the environment is one of the most difficult processes for the sewage media. Many procedures are utilized to eliminate or destroy the pollutants of sewage and Polluting gases. Some harmful methods are used strong oxidants which are unsafe. On the other hand, they were employed malicious procedures which can be generated serious problems. For example, air stripping which is (a procedure for the removing the unstable organic compounds from surface water or groundwater) changes water pollution to the air pollution. In addition, carbon adsorption is used for generation of a harmful solid which should be destroyed. In the one of the weaknesses processes, the pollutants are not damaged, but moved from one phase to another. Therefore, all procedures for removing organic pollutants should be replaced with methods have less harm on the environment [10-16].

The reaction with low rate of metallic oxide photocatalysis in the downgrade reactions needs to the synthesis of new photocatalysts. Thus, many researchers tried to optimize different properties such as crystalline structure, particle size, band gap, surface area, and different beds. Synthesis of nano particles is the best method to increase the surface of a photocatalyst, the reactive sites on its surface. In order to increase the active centers of a catalyst, it can be covered on a stabilizer such as silica [17-20]. The use of ultraviolet light for destroying pollutants by photocatalysts is a limitation for industry. Since the photocatalysts are semiconductor that can be overcome by reducing the band gap. A method for decreasing the band gap is putting up metals such as platinum, vanadium, silver *etc.* into the structure of photocatalysts [21-26].

In this work, the preparation of two nano-photocatalysts: ZnO/SiO₂ and Pt-ZnO/SiO₂ have been reported[27]. Also, the photocatalytic decomposition of Malachite green oxalate as an organic dye pollutant using two photocatalysts under UV-Vis light irradiation has been studied.

Experimental

All materials used in this work were purchased from Merck and used without modification. The crystal phase and particle size of the synthesized products were confirmed by X-ray diffraction (XRD) using FK60-04 with Cu K α radiation ($\lambda = 1.54 \text{ \AA}$), and with instrumental setting of 35 kV and 20 mA. The morphology of the nanostructures was observed by emission scanning electron microscopy (SEM, PHILIPS-XL ϕ 30). Fourier transform infrared (FT-IR) spectra were recorded by SHIMADZU-840S spectrophotometer using KBr pellet. BET analysis was carried out with QUANTASORB. UV-Vis Diffuse Reflectance Spectra (DRS) were obtained for the dry-pressed disk samples using a UV-Vis spectrophotometer (SHIMADZU-2550). The amount of degradation of Malachite Green was investigated by measuring the adsorption intensity of remained Malachite Green in the solution by means of UV-Vis spectroscopy (SHIMADZU-2550).

Preparation of ZnO nanoparticles

A solution of 5 mmol zinc acetate dihydrate in 30 mL absolute ethanol was added to a solution of surfactant CTAB ($\text{Zn}(\text{Ac})_2 \cdot 2\text{H}_2\text{O}$ to CTAB molar ratio was equal to 1) in 30 mL of absolute ethanol under stirring. For obtaining the pH ~ 10 in solutions, 20 mL of NaOH (0.3M) solution was added to the above solution under continuous stirring. The new solution was kept in a water bath at 70 °C for 2 h. It was observed that the solution started precipitating after one hour in water bath. After cooling the system to room temperature, the precipitate was separated by centrifugation, washed with absolute ethanol and deionized water for several times. The powder was dried under vacuum at 70 °C for 10 h. Finally, the nanoparticles were calcined at 750 °C for 3 h.

Preparation of nano-photocatalyst ZnO/SiO₂

The pH of suspension containing 0.01 mole ZnO (20 ml) was reached to 9-10 by adding NaOH solution (0.3 M). After stirring (10 h), the mixture was refluxed at 70 °C until stable zinc hydroxide sols were produced. After the reflux was finished, some tetraethyl orthosilicate was added to the previous mixture at the same temperature to achieve the mole ratio of 30/70 (zinc/silicon). The formed sol was kept in the vacuum at room temperature for two days. Then it was calcined at 400 °C for 3 h.

Preparation of Pt-loaded ZnO/SiO₂

5mmol ZnO/SiO₂ were stirred in 50 mL of methanol aqueous solution (1%wt) containing 1 mL of H_2PtCl_6 solution (0.4M) and irradiated by two lamp (30 W Hg) for 20 h. During the irradiation, H_2PtCl_6 was reduced and converted to Pt metal particles on ZnO/SiO₂ catalysts to form Pt-loaded (1

wt %) ZnO/SiO₂. After filtering and washing photocatalysts with distilled water, the photocatalysts were dried at 200 °C for 2 h to remove the excess methanol adsorbed on the catalysts surface.

Degradation of malachite green dye using the synthesized catalysts

Suspensions containing 150 ml of 10 ppm malachite green dye together with ZnO/SiO₂ and Pt-ZnO/SiO₂ catalysts with a concentration of 0.2, 0.3, and 0.4 g/L (pH of the suspensions was stabilized at 3, 4, 5, and 6), a magnetic stirrer, and an air flow which was blown into a reactor through a tube to uniform the environment were used in each experiment. The reactor consisted of two tungsten lamps with two range of wavelength which wavelength 220-230nm was used for irradiation at UV range and 500-700nm for irradiation at visible range. It should be noted that in the experiment conditions are optimized basis as the amount of catalyst, the environment pH, and the irradiation time. The optimized irradiation time is 120 min. Before irradiation, all solutions were stirred for 30 min in the dark to balance absorption and desorption of pollutants on the catalyst surface. A UV-Vis spectrophotometer was used to study the degradation of pollutants. Thus the absorption spectra of the samples were measured at certain intervals and the amount of the pollutant removal or its conversion to another substance was evaluated by the decrease in intensity of the relevant absorption peak.

Results and discussion

Structural analysis of the catalysts

The XRD patterns of ZnO nanoparticles (a), ZnO@SiO₂ (b) and Pt-loaded ZnO/SiO₂ nanophotocatalysts (c) are shown in Figure 1(a-c). All peaks can be well indexed to wurtzite type crystal structure (hexagonal phase) with lattice constants of $a=0.32495$ nm and $c=0.52069$ nm (JCPDS, No.36-1451)[26,27]. No other crystalline phases were found in the XRD patterns, indicating the high purity of the products. The crystallite sizes can be calculated using *Scherrer's* equation: $D= 0.9 \lambda / (\beta \cos\theta)$ where λ is the X-ray wavelength (1.54Å), β is the full-width at half-maximum intensity of the diffraction line and θ is the diffraction angle. The crystallites sizes are estimated to be around 32 nm. Also, the surface area was obtained 358m²/g for ZnO catalyst calcined at 750°C temperature from BET analysis.

In Figure 1b a board new peak is appeared at ~22° diffraction angles, which shows the presents of amorphous SiO₂ in the sample [27, 28].

Figure 1c shows the XRD pattern of Pt doped ZnO/SiO₂ sample. In this Figure two new peaks are appeared at 40.05° and 46.52° diffraction angles, which can be indexed to platinum (JCPDS, No. 01-1194). Therefore, the Pt-loaded ZnO/SiO₂ is carried out successfully.

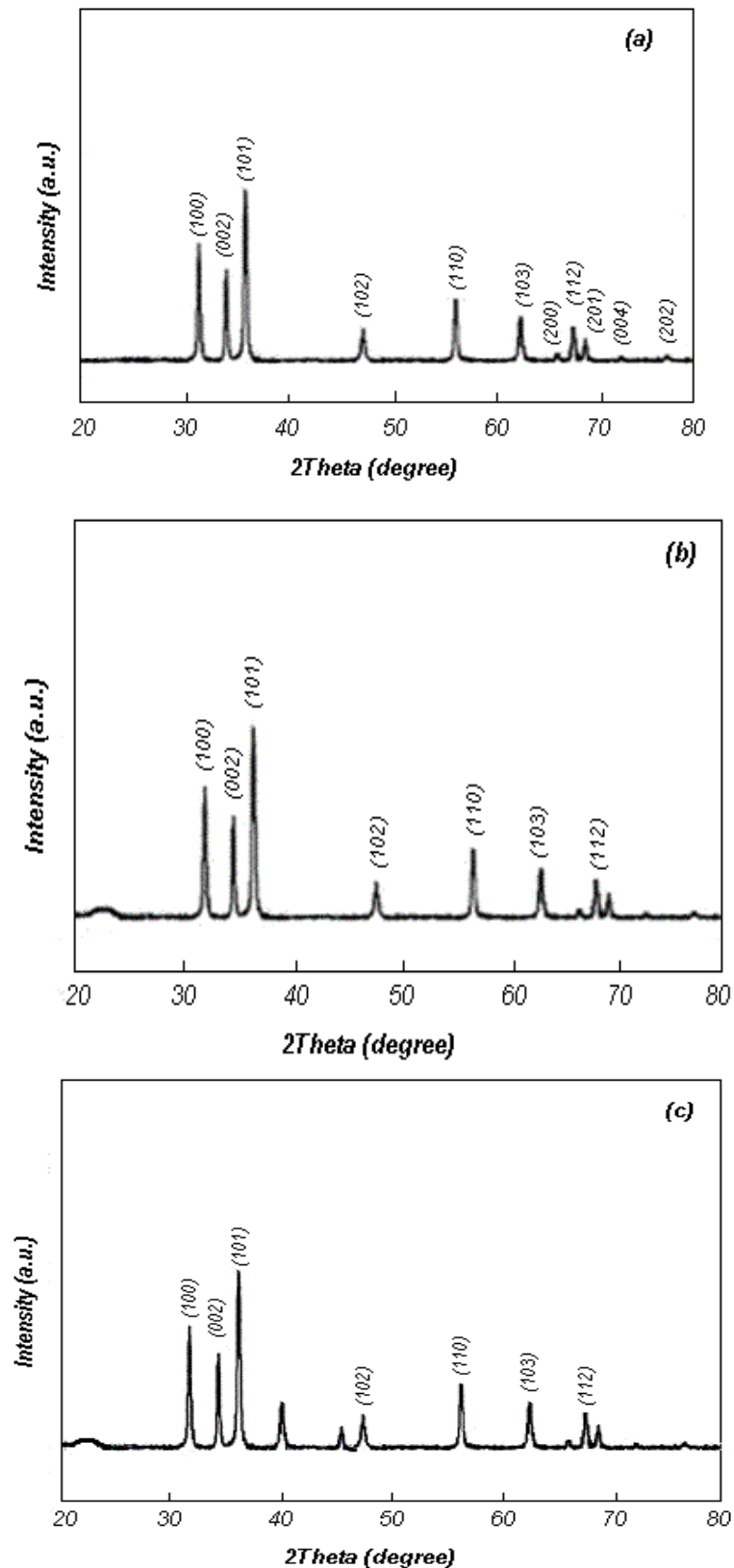


Figure1. XRD patterns of (a) ZnO, (b) ZnO/SiO₂, and (c) Pt - ZnO/SiO₂ samples.

The FT-IR spectra of ZnO and ZnO/SiO₂ nanoparticles are shown in Figure 2(a-b). The vibrational peaks in the range of 3600-3650 cm⁻¹ and 1600-1650 cm⁻¹ can be attributed to the stretching and

bending vibrations of structural hydroxyl groups of the adsorbed water. The peak in the range of $420-450\text{ cm}^{-1}$ can be associated to the stretching vibration mode of Zn-O [27, 29-30]. The peaks in the ranges of $1050-1110\text{ cm}^{-1}$ and $750-800\text{ cm}^{-1}$ in Figure 2b are corresponded to the asymmetric and symmetric stretching vibration modes of Si-O-Si, respectively. However these peaks are absent in Figure 2a. The peak which is appeared at $440-480\text{ cm}^{-1}$ is due to the bending vibration mode of Si-O-Si [27, 31]. These results are in agreement with the results of XRD patterns.

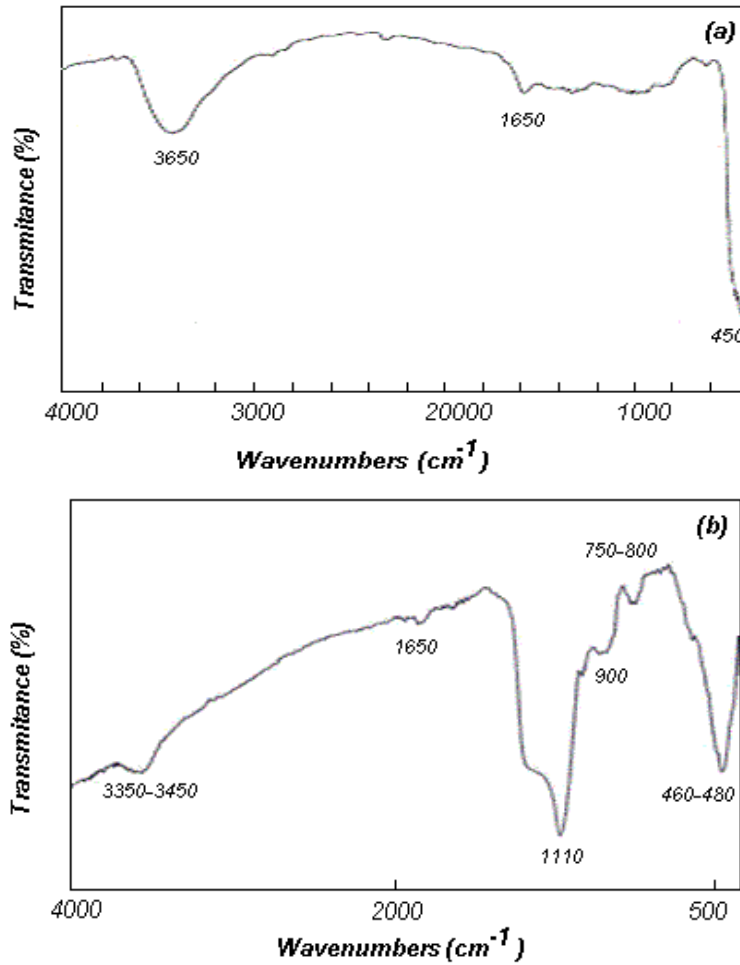


Figure 2. FT-IR spectra of (a) ZnO and (b) ZnO/SiO₂ samples.

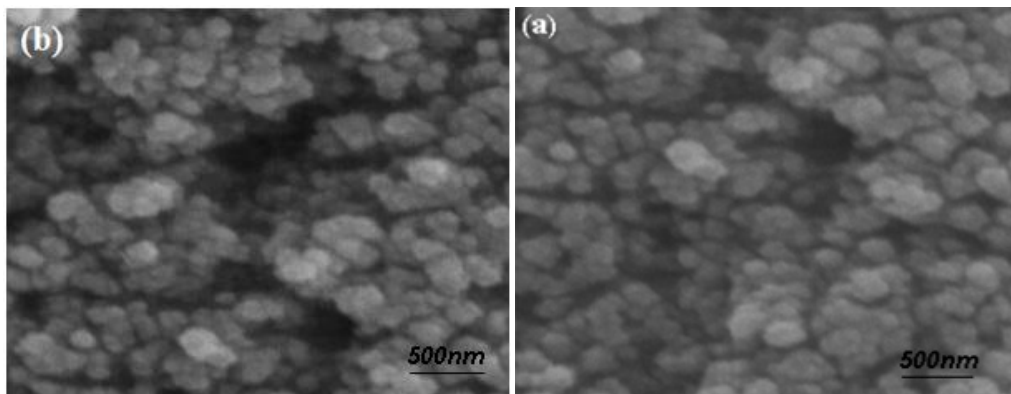


Figure 3. SEM images of (a) bare ZnO, and (b) Pt- ZnO/SiO₂ nanoparticles.

The morphology of the products was observed by SEM images. The SEM images of ZnO, and Pt-doped ZnO/SiO₂ nanoparticles are shown in Figure 3(a-b), respectively.

Photocatalytic activity

Degradation of Malachite green dye using ZnO/SiO₂ and Pt-ZnO/SiO₂ photocatalysts under UV irradiation

Malachite green dye has three absorption bands at wavelengths of 617, 424, and 316 nm which are related to the electron transfers of $\pi \rightarrow \pi^*$ of the aromatic ring induced by attached N-methyl groups and $n \rightarrow \sigma^*$ and $\sigma \rightarrow \sigma^*$ of the aromatic ring, respectively (Figure 4). The mechanism of malachite green dye degradation performs through conjugated structure degradation or dimethyl removal. If decrease was seen in the absorption intensity during the reaction with a shift of the absorption peak (617 nm) toward shorter wavelengths, the reaction proceeds through dimethyl removal. The reason for this shift is the removal of *N, N*-dimethyl chromophore which is an electron donor and its gradual elimination during degradation results in the absorption range of aromatic system to shift toward shorter wavelengths. If the maximum peak intensity gradually decreases without any shift in the absorption wavelength, the reaction performs through the conjugated structure degradation [32].

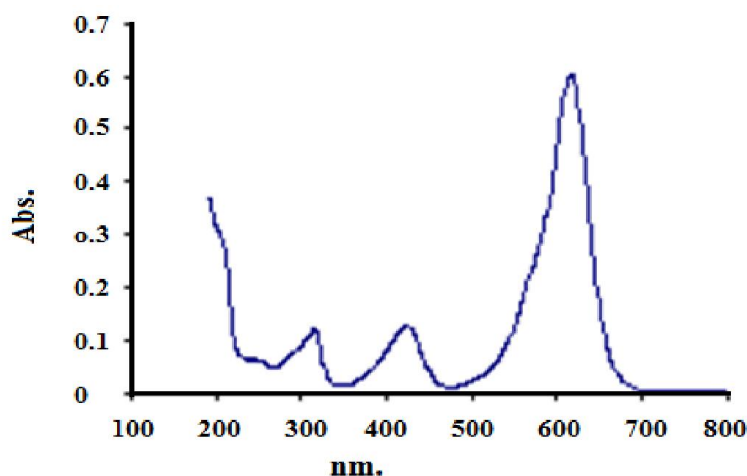


Figure 4. UV-Vis spectrum of malachite green (10 ppm) .

Figures 5-8 show the degradation of malachite green dye at pH range of 3-6 on ZnO/SiO₂ (0.3 g/L). As seen in the general pattern of the spectra, the amount of absorption of malachite green dye on this catalyst is directly related to the pH increment. To justify this increase, it can be noted that the pH_{zcp} of the catalyst is 8.7 and at pH below pH_{zcp} the catalyst surface is positively charged, thus it has more potential to attract negatively charged ions. By increasing pH and its approximation to

pH_{zpc} , negative charges are gradually increased on the catalyst surface, and therefore, malachite green dye with an unstable positive charge is better absorbed by the catalyst.

Along with the degradation progress and reduction of the maximum absorption wavelength intensity, a shift toward lower wavelengths can be seen in all UV-Vis absorption spectra at $\text{pH}=3-6$ that is shown in the Figures of malachite green dye degradation. The reason for this shift is the elimination of *N,N*-dimethyl chromophore. This chromophore is an electron donor, thus following the process; the absorption wavelength of the aromatic system is shifted toward higher wavelengths. After its gradual elimination during degradation, the absorption range of the aromatic system is shifted toward shorter wavelengths.

The degradation process and 30 minutes after beginning of the reaction, some peaks were quickly appeared in the ranges of 350-370 and 230-250 nm. The peak at 350-370 nm cannot be attributed to a stable product during the reaction. Because of as is shown in Figures 5- 8 and in particular Figure 7, this peak is more like a shoulder rather than a clear peak, representing the generation of an intermediate. After an hour and degradation of the intermediate, no specific shift was appeared at 350-370 nm, concluding that its degradation is not associated with the removal of chromophore. The intermediate reaches its maximum amount one hour after initiation of the reaction and then its resorption and destruction begins following depletion of the catalyst active centers. The degradation rate of this intermediate is directly related to the degradation rate of malachite green (rate of the maximum peak disappearance). Because of faster degradation of malachite green, deplete more the catalyst active centers which enable them to absorb the intermediates. At $\text{pH} = 5$, the peak is completely removed over two hours. The other peak in the range 230-250 nm with a fluctuating value (adsorption and desorption), is likely to be the products of degradation. According to the degradation reactions of malachite green in the presence of ZnO/SiO_2 (0.3 g/L) at $\text{pH}=3-6$, the highest photocatalytic activity of ZnO/SiO_2 was realized at $\text{pH}=5$.

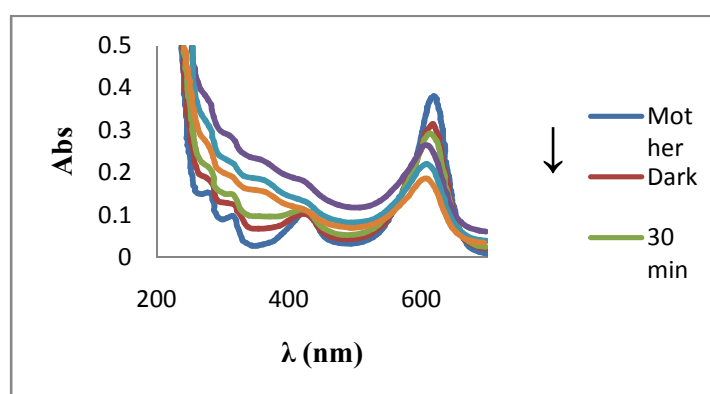


Figure 5. Photodegradation of MG on bare ZnO/SiO_2 photocatalyst at $\text{pH}=3$.

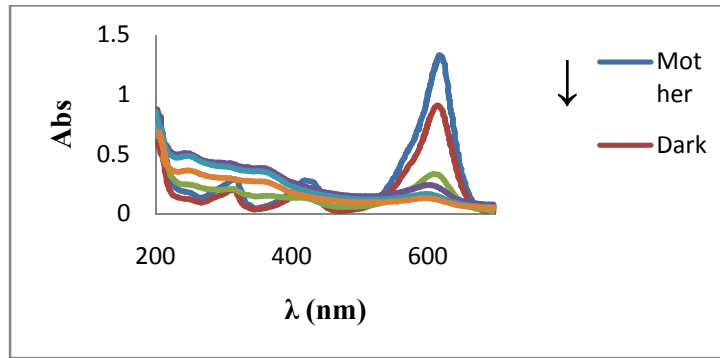


Figure6. Photodegradation of MG on bare ZnO/SiO₂ photocatalyst at pH=4.

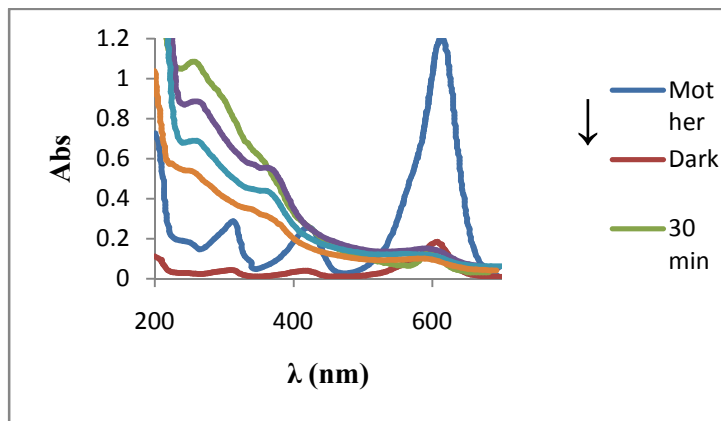


Figure7. Photodegradation of MG on bare ZnO/SiO₂ photocatalyst at pH=5.

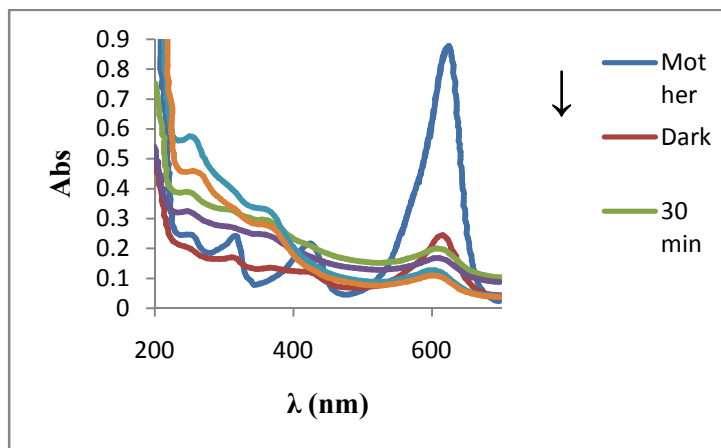


Figure8. Photodegradation of MG on bare ZnO/SiO₂ photocatalyst at pH=6.

The optimum amount of ZnO/SiO₂ and appropriate pH of the solution for degradation of 150 ml malachite green dye with a concentration of 10 ppm were obtained 0.3 g/L and 5, respectively, (Tables 1 and 2).

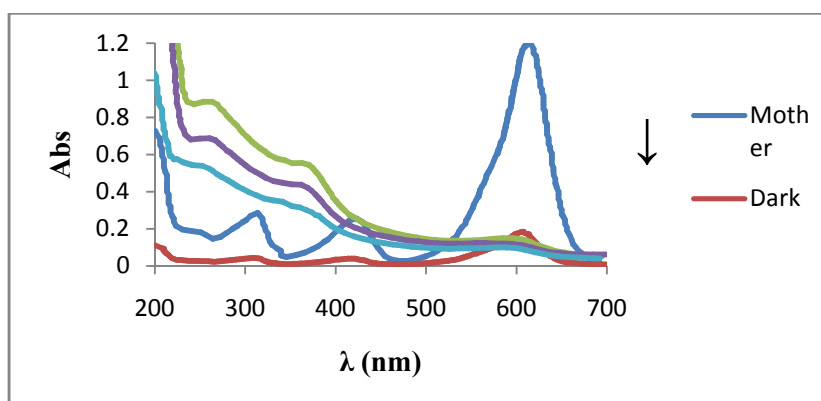
Table 1. The results of photodegradation of MG (%) on ZnO/SiO₂ photocatalyst (0.2, 0.3 and 0.4 g/L) at pH=5.

The amount of ZnO/SiO ₂ (g/L), pH=5	The degradation of MG (%)
0.2	73.2
0.3	99.5
0.4	75.2

Table 2. The results of photodegradation of MG (%) on ZnO/SiO₂ photocatalyst (0.3 g/L) at pH=3, 4, 5, and 6.

pH (The amount of ZnO/SiO ₂ = 0.3 g/L)	The degradation of MG (%)
3	24.3
4	65.2
5	99.5
6	69.2

Figure 9 shows the variation of malachite green spectrum treated through heterogeneous photocatalysis with 0.3 g/L Pt-ZnO/SiO₂ at pH= 5 (optimal conditions) for 90 minutes. The reduction rate of maximum absorption and the difference of dye concentration are completely clear from the spectra. As seen, the initial amount of the dye absorption in this catalyst is more than ZnO/SiO₂, while UV-Vis spectra pattern of both pure and doped catalysts are like each other. Higher dye adsorption of Pt-ZnO/SiO₂ is due to low pH_{zpc} of this catalyst (4.2). In addition, change of the dye concentration from spectra displays that the destructive reaction of malachite green on Pt-ZnO/SiO₂ occurs faster than ZnO/SiO₂ under UV irradiation. This is due to the presence of platinum. As we know, doped metal ions affect optical activity through trapping electrons or holes and altering the reproduction rate of e^-/h^+ . These results are similar to the results of the degradation of malachite green by the V₂O₅-ZnO/SiO₂ photocatalyst [33]. This similarity of results can be due to the same shift of ZnO/SiO₂ band gap for both of photocatalysts.

**Figure 9.** Photodegradation of MG on Pt-ZnO/SiO₂ photocatalyst at pH=5.

Degradation of Malachite Green dye with ZnO/SiO₂ and Pt-ZnO/SiO₂ photocatalysts under visible light

Since ZnO/SiO₂ has a large band gap, it is not able to perform photocatalysis reaction in the visible light. The band gap of ZnO/SiO₂ and Pt-ZnO/SiO₂ were calculated by UV-Vis diffuse reflectance spectra (Figure 10) and equation 1. The band gap values are obtained around 3.20 and 2.19 eV for ZnO/SiO₂ and Pt-ZnO/SiO₂, respectively.

$$E = hc/\lambda, \text{ (Eq.1)}$$

Where λ is estimated from shoulder or peak of the spectra correspond to the fundamental absorption edges in the samples. h is Planck constant, c is the speed of light and E is energy ($1\text{eV} = 1.602 \times 10^{-19}$ J). Figure 11 shows changes in the absorption spectra of malachite green by Pt-ZnO/SiO₂ under visible light. As seen in this figure, changes in the absorption spectra of malachite green catalyst by Pt-ZnO/SiO₂ under visible light is similar to the degradation mechanism under UV radiation. The reaction is continued for about 120 min and malachite green is completely degraded by Pt-ZnO/SiO₂ under visible light. Given the band gap distance of ZnO/SiO₂ (3.20 eV), the activity of ZnO/SiO₂ in the visible light is minimal, while doping of Pt in ZnO network displaced the band gap toward longer wavelengths (visible light) and increased the photocatalysis activity in the range of visible light. The UV-vis diffuse reflectance spectra of catalysts (Figure 10) confirm the reduction of Pt-ZnO/SiO₂ band gap compared to ZnO/SiO₂.

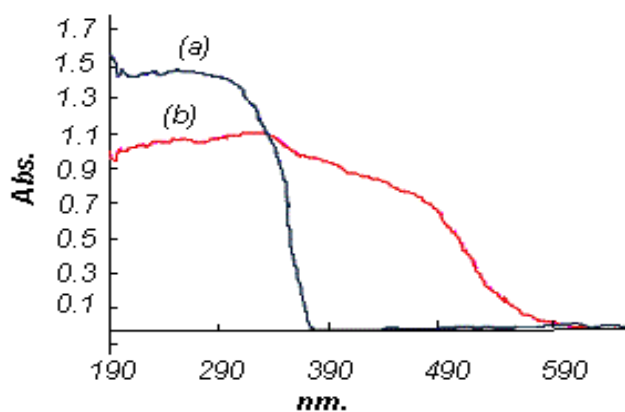


Figure 10. UV-Vis Diffuse Reflectance Spectra of (a) ZnO/SiO₂, and (b) Pt-ZnO/SiO₂ nanoparticles.

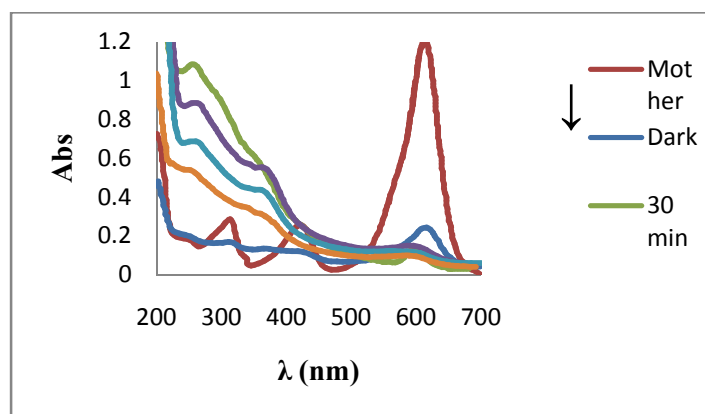


Figure 11. Photodegradation of MG on Pt-ZnO/SiO₂ photocatalyst at pH=5 (under visible light).

Conclusion

ZnO/SiO₂ nanocomposite was produced using sol-gel method. Also, platinum particles were successfully loaded on this nano-photocatalyst by photoreductive method. The results were shown that the amount of adsorbed malachite green dye on this catalyst is directly related to the pH increment. The optimum amount of ZnO/SiO₂ and optimized pH of the solution for degradation of malachite green dye (150 ml, 10 ppm) were obtained 0.3 g/L and 5, respectively. In optimal conditions, change of dye concentration from spectra shows that the destructive reaction of malachite green on Pt-ZnO/SiO₂ occurs faster than ZnO/SiO₂ under UV irradiation. Moreover, the activity of ZnO/SiO₂ in the visible light is minimal, while doping of Pt in ZnO network displaced the band gap toward longer wavelengths (visible light) and increased the photocatalysis activity in the range of visible light. The result of the photocatalytic test shows that Pt-ZnO/SiO₂ may be an extremely viable adsorbent for application in the treatment of water and industrial wastewater contaminated with dyes.

Acknowledgment

This article was extracted from the project entitled: “Doping of Pt on ZnO/SiO₂ and Photodegradation of industrial wastewaters by Pt-ZnO/SiO₂ Nanophotocatalyst”. Financial support for this project was provided by Islamic Azad University Firoozkooh branch.

References

- [1] S. S. Mao, S. Shen, *Nat. Photonics*, 7, 944 (2013).
- [2] A. O. Ibhaddon, P. Fitzpatrick, *Catalysts*, 3, 189 (2013).
- [3] S. Shen, C. Kronawitter, G. Kiriakidis, *J. Materiomics*, 3, 1 (2017).
- [4] S. Sontakke, J. Modak, G. Madras, *Chem. Eng. J.*, 165, 225 (2010).
- [5] E. G. L. Oliveiraa, J. J. Rodrigues, H. P. Oliveiraa, *Chem. Eng. J.*, 172, 96 (2011).

- [6] A. M. Luis, M. C. Neves, M. H. Mendonc, O. C. Monteiro, *Mater. Chem. Phys.*, 125, 20 (2011).
- [7] C. N. Uma, M. Priya, *Int. J. eng. Sci. manage. Res.*, 2, 114 (2015).
- [8] J. J. Lopez-Penalver, M. Sanchez-Polo, C.V. Gomez-Pacheco, J. Rivera-Utrilla, *J. Chem. Technol. Biotechnol.*, 85, 1325 (2010).
- [9] J. Liqiang, S. Xiaojun, S. Jing, C. Weimin, X. Zili, D. Yaoguo, F. Honggang, *Sol. Energy. Mater. Sol. Cells.*, 79, 133 (2003).
- [10] S. Gharibe, L. Vafayi, S. Afshar, *J. Appl. Chem. Res.*, 9, 103 (2015).
- [11] H. Shu, J. Xie, H. Xu, H. Li, Z. Gu, G. Sun, Y. Xu, *J. Alloy. Compd.*, 496, 633 (2010).
- [12] T. N. Ramesh, A. Ashwini, D. V. Kirana, *J. Appl. Chem. Res.*, 10, 35 (2016).
- [13] N. P. Mohabansi, V. B. Patill, N. Yenkie, R. Rasayan, *J. Chem.*, 4, 814 (2011).
- [14] R. Slama, F. Ghribi, A. Houas, C. Barthou, L. E. Mir, *Int. J. Nanoelect. Mater.*, 3, 133 (2010).
- [15] A. F. Comanescu, M. Mihaly, A. Meghea, *U.P.B. Sci. Bull. Series. B.*, 74(2), 49 (2012).
- [16] L. Vafyi, S. Gharibe, *Iran. J. Catal.*, 5, 365 (2015).
- [17] D.V. Demydov, Nanosized Alkaline Earth Metal Titanates: Effects of Size on Photocatalytic and Dielectric Properties, Kansas State University Manhattan Kansas (2006).
- [18] J. Li, D. Guo, X. Wang, H. Wang, H. Jiang, B. Chen, *Nanoscale. Res. Lett.*, 5, 1063 (2010).
- [19] S. Baskoutas, A. F. Terzis, *J. Appl. Physic.*, 99, 013708 (2006).
- [20] C. Chen, J. Liu, P. Liu, B. Yu, *Adv. Chem. Eng. Sci.*, 1, 9 (2011).
- [21] S. Kant, A. Kumar, *Adv. Mat. Lett.*, 3, 350 (2012).
- [22] F. J. Sheini, J. Singh, O. N. Srivasatva, D. S. Joag, M. A. More, *Appl. Surf. Sci.*, 256, 2110 (2010).
- [23] S. J. Pearton, I. E. Fellow, D. P. Norton, M. P. Ivill, A. F. Hebard, M. J. Zavada, W. M. Chen, I. A. Buyanova, *Trans. Electron. Devic.*, 54, 1040 (2007).
- [24] M. Qamar, M. Muneer, *Desalination*, 249, 535 (2009).
- [25] M. Faiz, N. Tabet, A. Mekki, B. S. Mun, Z. Hussain, *Thin. Solid. Films*, 515, 1377 (2006).
- [26] J. Kim, K. Yong, *J. Nanopart. Res.*, 14, 1033 (2012).
- [27] S. Gharibe, L. Vafayi, S. Afshar, *J. Indian. Chem. Soci.*, 91, 527 (2014).
- [28] A. İ. Vaizoğullar, A. Balcı, *Int. J. Res. Chem. Environ.*, 4, 161 (2014).
- [29] Z. R. Khan, M. S. Khan, M. Zulfequar, M. S. Khan, *Mater. Sci. Appl.*, 2, 340 (2011).
- [30] R. N. Gayen, K. Sarkar, S. Hussain, R. Bhar, A. K. Pal, *Ind. J. Pure. Appl. Phys.*, 49, 470 (2011).
- [31] F. Li, X. Huang, Y. Jiang, L. Liu, Z. Li, *Mater. Res. Bull.*, 44, 437 (2009).
- [32] Y. Li, G. Lu, S. Li, *J. Photoch. Photobio. A: Chem.*, 152, 219 (2002).
- [33] S. Gharibe, L. Vafayi, S. Afshar, *J. Indian. Chem. Soc.*, 92, 337 (2015).